Image Cover Sheet

CLASSIFICATION	SYSTEM NUMBER
UNCLASSIFIED	499617

TITLE

APPROXIMATIONS TO EXTINCTION FROM RANDOMLY ORIENTED CIRCULAR AND ELLIPTICAL CYLINDERS

System Number:

Patron Number:

Requester:

Notes:

DSIS Use only:

Deliver to:

Approximations to extinction from randomly oriented circular and elliptical cylinders

G. R. Fournier and B. T. N. Evans

Analytic approximations to the extinction efficiency, Q_{ext}, are given for oriented and randomly oriented circular infinite cylinders based on anomalous diffraction. The results are compared with the exact code. These results are further generalized to randomly oriented elliptical cylinders. With the use of the formulas, Q_{ext} can be evaluated over 10^4 times faster than with the exact code. This approximation is valid for complex refractive indices $m = n - ik$, where $1 \le n \le \infty$ and $0 \le k \le 3$, aspect ratios from 1 to 4, and modest to large particle sizes. The accuracy and limitations of these formulas are discussed.
Key words: Extinction, scattering, aerosols, cylinders.

1. Introduction

The immediate objective of this study is to reduce significantly the computational burden in calculating the extinction from cylindrical particles. The conventional calculation with randomly oriented infinite cylinders can require large computation times, especially for polydispersions, larger particle sizes, and refractive indices. The approximations presented here obviate the need for such computations, and thus they allow for the exploration of the effects of cylindrical particles on the performance of electro-optical and millimeter wave systems in obscurants, ice clouds, and hydrosols.

We have previously presented[1] an analytic approximation to Q_{ext} for randomly oriented spheroids. This research applies to particles with $n > 1$ and $k > 0$ for arbitrary sizes and aspect ratios. The basic approach was to orthogonalize as much as possible the scattering physics into well-defined regimes. The large-particle regime was successfully modeled by anomalous diffraction and edge (Fock) terms. Here we take the same basic approach but apply it to randomly oriented cylinders instead.

The report is organized as follows. Section 2 develops the extinction formula. Section 3 contains comparisons of this approximation to the exact code from IPHASE,[2] Section 4 extends the anomalous diffraction approach and explores the ramifications, and Section 5 develops and discusses approximations to randomly oriented elliptical cylinder extinction. The final section, Section 6, gives the conclusions and limitations.

The authors are with the Defense Research Establishment Valcartier, Courcelette, Quebec G0A 1R0, Canada.

Received 13 June 1995; revised manuscript received 24 January 1996.

2. Development of the Extinction Formula

The physics and the structure of the extinction formula for randomly oriented cylinders are developed here. Only medium to large size parameters are considered; hence these formulas will not apply in the small particle or Rayleigh region.

A. Anomalous Diffraction Term

The anomalous diffraction approach was first discussed by Van de Hulst[3] for spheres. Furthermore, it was extensively developed for oriented infinite cylinders by Stephens.[4] One derives the anomalous diffraction formula by assuming that the incident plane wave is not significantly skewed as it passes through the scattering object and that, to first order, the effect of the scatterer is to delay locally the phase of the wave and attenuate its amplitude.[3] The strict limit of validity of the formula is therefore the region where $(n - 1) \ll 1$. The cylinder is, in effect, treated as a slit normal to the incident wave possessing a spatially dependent phase and amplitude. The Fraunhofer pattern at infinity is then derived and Q_{ext} is evaluated from the standard relations. For a cylinder with its axis oriented at an angle θ with respect to the direction of the incident radiation, this procedure leads immediately to the following formula[4]:

$$Q_{ad} = \pi \mathrm{Re}[\mathbf{H}_1(\omega) + iJ_1(\omega)], \quad (1)$$

where ω is given by

$$\omega = 2(m - 1)x/\sin\theta, \quad (2)$$

the complex refractive index is $m = n - ik$, and x is the size parameter. In Eq. (1), $\mathbf{H}_1$ and J_1 are the first-order Struve and Bessel functions, respectively. These are well defined in Ref. 5. Clearly, when the index is real only the first term in Eq. (1) appears.

For random orientation the angle averaging gives

$$\overline{Q}_{\mathrm{ad}} = \frac{\int_0^{\pi/2} Q_{\mathrm{ad}} \sin^2\theta \mathrm{d}\theta}{\int_0^{\pi/2} \sin^2\theta \mathrm{d}\theta}, \tag{3}$$

$$= 4\,\mathrm{Re}\left[\int_0^{\pi/2} \mathbf{H}_1(\omega)\sin^2\theta \mathrm{d}\theta + i\int_0^{\pi/2} J_1(\omega)\sin^2\theta \mathrm{d}\theta\right]. \tag{4}$$

The first term in Eq. (4) can be analytically integrated as follows:

$$4\int_0^{\pi/2} \mathbf{H}_1\left(\frac{\rho}{\sin\theta}\right)\sin^2\theta \mathrm{d}\theta = 2\int_1^{\infty} \frac{\mathbf{H}_1(\rho\sqrt{z})\mathrm{d}z}{z^2\sqrt{z-1}}, \tag{5}$$

by the use of simple transform $z = 1/\sin^2\theta$. This integral appears as a special case of Eq. 2.7.4.6 in Ref. 6. We initially use a more general approach for later purposes. We solve it by using a general hypergeometric form of the above Weyl-type integral. From Ref. 7, p. 417, formula 20.5 (2), we have

$$\int_1^{\infty} x^{-\eta}(x-1)^{\sigma-1} G_{pq}^{mn}\left(\alpha x\middle|\begin{matrix}\alpha_p\\ \beta_q\end{matrix}\right)\mathrm{d}x = \Gamma(\sigma) G_{p+1,q+1}^{m+1,n}\left(\alpha\middle|\begin{matrix}\alpha_p, \eta\\ \eta-\sigma, \beta_q\end{matrix}\right), \tag{6}$$

where G_{pq}^{mn} is the Meijer G function. The Struve function is represented by the following G function[8]:

$$\mathbf{H}_1(x) = G_{1,3}^{1,1}\left(\frac{x^2}{4}\middle|\begin{matrix}1\\ 1, 1/2, -1/2\end{matrix}\right). \tag{7}$$

Using Eqs. (7) and (6) in (5), we get

$$2\int_1^{\infty} \frac{\mathbf{H}_1(\rho\sqrt{z})\mathrm{d}z}{z^2\sqrt{x-1}} = 2\int_1^{\infty} z^{-2}(z-1)^{-1/2} \times G_{1,3}^{1,1}\left(\frac{\rho^2 z}{4}\middle|\begin{matrix}1\\ 1, 1/2, -1/2\end{matrix}\right)\mathrm{d}z,$$

$$= 2\Gamma\left(\frac{1}{2}\right) G_{2,4}^{2,1}\left(\frac{\rho^2}{4}\middle|\begin{matrix}1, 2\\ 3/2, 1, 1/2, -1/2\end{matrix}\right). \tag{8}$$

Following Ref. 8, p. 230, formula 6.5 (1), one can reduce the above G function, giving

$$2\Gamma\left(\frac{1}{2}\right) G_{2,4}^{2,1}\left(\frac{\rho^2}{4}\middle|\begin{matrix}1, 2\\ 3/2, 1, 1/2, -1/2\end{matrix}\right) = 2\rho^2\left[\frac{2}{3} - \frac{\rho\pi}{16}\,{}_1F_2\left[\begin{matrix}1/2\\ 2, 3\end{matrix}\middle|\frac{-\rho^2}{4}\right]\right], \tag{9}$$

Equation (9) can be directly obtained by Eq. 2.7.4.6 of Ref. 6 as mentioned above. One can further simplify the ${}_1F_2$ in Eq. (9) by expressing it in terms of Bessel functions of the first kind. Formulas to accomplish this can be found,[6] finally giving

$$2\int_1^{\infty} \frac{\mathbf{H}_1(\rho\sqrt{z})\mathrm{d}z}{z^2\sqrt{z-1}} = \frac{4}{3}\rho^2\left\{1 - \frac{\rho\pi}{4}\left[J_0^2\left(\frac{\rho}{2}\right) - \frac{2}{\rho}J_0\left(\frac{\rho}{2}\right)J_1\left(\frac{\rho}{2}\right) + \left(1 - \frac{2}{\rho^2}\right)J_1^2\left(\frac{\rho}{2}\right)\right]\right\}. \tag{10}$$

Equation (10) is the full solution to Q_{ad} for real indices. It is remarkably simple and is readily computable.

The second term in Eq. (4) is treated as follows:

$$4i\int_0^{\pi/2} J_1\left(\frac{\rho}{\sin\theta}\right)\sin^2\theta \mathrm{d}\theta = 2i\int_1^{\infty} \frac{J_1(\rho\sqrt{z})\mathrm{d}z}{z^2\sqrt{z-1}}. \tag{11}$$

This integral is not explicitly in the integral tables so we use Eq. (6) and the G function representation of J_1:

$$J_1(x) = G_{0,2}^{1,0}\left(\frac{x^2}{4}\middle|\begin{matrix}-\\ 1/2, -1/2\end{matrix}\right). \tag{12}$$

This gives

$$2i\int_1^{\infty} \frac{\mathbf{J}_1(\rho\sqrt{z})\mathrm{d}z}{z^2\sqrt{z-1}} = 2i\int_1^{\infty} z^{-2}(z-1)^{-1/2} \times G_{0,2}^{1,0}\left(\frac{\rho^2 z}{4}\middle|\begin{matrix}-\\ 1/2, -1/2\end{matrix}\right)\mathrm{d}z,$$

$$= 2i\Gamma\left(\frac{1}{2}\right) G_{1,3}^{2,0}\left(\frac{\rho^2}{4}\middle|\begin{matrix}2\\ 3/2, 1/2, -1/2\end{matrix}\right). \tag{13}$$

This G function can be shown to be of the logarithmic type, which means that no finite expression in terms of hypergeometric functions can be obtained. However, it can be formally expressed as an infinite series, giving for Eq. (13) the following:

$$2i\Gamma\left(\frac{1}{2}\right) G_{1,3}^{2,0}\left(\frac{\rho^2}{4}\middle|\begin{matrix}2\\ 3/2, 1/2, -1/2\end{matrix}\right) = \frac{i\rho}{4}\left\{4 + \frac{\rho^2}{4}\ln\frac{\rho^2}{4}\,{}_1F_2\left[\begin{matrix}1/2\\ 2, 3\end{matrix}\middle|-\frac{\rho^2}{4}\right] + \sum_{k=0}^{\infty}\left(-\frac{\rho^2}{4}\right)^{2k+1}\frac{(1/2)_k}{(2)_k(3)_k k!}\left[3\psi(k+1) - \psi\left(k - \frac{1}{2}\right) + \frac{2}{1-2k} + \frac{2}{1+k} + \frac{1}{2+k}\right]\right\}, \tag{14}$$

Here $\psi(z)$ is the digamma function and $(a)_k$ is the Pochhammer symbol.[5] Because of the slow convergence of the sum in Eq. (14), even for modestly large ρ, it is not of great computational value. Therefore another simpler approximation is required.

We go back to the physical level. When there is no absorption, there is constructive and destructive interference. This produces the familiar oscillations in Q_{ext}. This is well described by Eq. (10). Absorption affects the interference spatially by reducing the amplitude of the partial waves inside the particle. This has the effect of damping the magnitude of the oscillations in Q_{ext}. For very large absorptions the particle is opaque, no waves are transmitted, and hence, by Babinet's principle, $Q_{ext} = 2$. To first order we neglect the effect of the spatial dependence of absorption on the interference. We can do this by averaging $\exp(-2ky/\sin\theta)$ spatially and over angles. Here y is a cord length through the cylinder. This procedure unfortunately leads to another logarithmic G function of similar complexity as Eq. (14). In order to avoid this difficulty, we instead average absorption length $2ky/\sin\theta$ spatially and over angles. The resulting formula is strictly valid only in the limit of small absorption length. However, as soon as the damping of the interference term becomes significant, it contributes little to the extinction efficiency. The procedure therefore produces a negligible additional error even for moderate to large values of absorption length. The angular average is given by

$$\frac{\int_0^{\pi/2} (2ky/\sin\theta)\sin^2\theta\,d\theta}{\int_0^{\pi/2} \sin^2\theta\,d\theta} = \frac{8ky}{\pi}. \tag{15}$$

Then doing the spatial averaging to get the final averaged absorption length, λ, we have

$$\begin{aligned}\lambda &= \frac{2\int_0^x (8ky/\pi)dz}{2\int_0^x dz},\\ &= \frac{8k}{\pi x}\int_0^x (x^2 - z^2)^{1/2}dz,\\ &= 2kx.\end{aligned} \tag{16}$$

This simple average gives $\exp(-\lambda)$ as the approximate damping factor.

One can isolate the oscillating terms from Q_{ad} (for real m) by subtracting from it the constant Babinet term, which is 2. These can then be damped by $\exp(-\lambda)$ and then the Babinet term added back. Thus the approximation to Q_{ad}, including absorption, becomes

$$Q_{ad} \approx 2 + \exp(-2kx)\left(\frac{4}{3}\rho^2\left\{1 - \frac{\rho\pi}{4}\left[J_0^2\left(\frac{\rho}{2}\right) - \frac{2}{\rho}J_0\left(\frac{\rho}{2}\right)J_1\left(\frac{\rho}{2}\right) + \left(1 - \frac{2}{\rho^2}\right)J_1^2\left(\frac{\rho}{2}\right)\right]\right\} - 2\right), \tag{17}$$

where $\rho = 2(n-1)x$. Note that ρ is now always real.

B. Edge Effects

For a particle whose typical size is much larger than the wavelength, the edge cannot be treated as sharp and the effect of the curvature of the object must be included. Jones[9] has shown how to estimate these edge effects for convex bodies. As he clearly explains, near a glancing point the body will behave approximately like a cylinder with its axis perpendicular to the surface normal (at the glancing point) and the direction of propagation of the incident wave. The scattering and absorption from all such cylindrical sections can be integrated around the projection of the penumbral curve to give the total contribution of the edge effects to the extinction cross section. The projection is onto the plane normal to the incident ray direction. The energy scattered per unit length of the cylinder by the region on its surface around the glancing point is proportional to $c_{TE}R^{1/3}$ for the TE mode and $c_{TM}R^{1/3}$ for the TM mode, where R is the radius of curvature of the cylinder. Constants c_{TE} and c_{TM} are the first-order Fock terms. It can be shown that, for convex bodies, randomly oriented or illuminated by a randomly polarized beam, $(c_{TE} + c_{TM})/2 = c_e$, where c_e is a universal function of refractive index. Following Jones, we see that the edge contribution to the extinction efficiency of the body is

$$Q_{edge} = \frac{c_e}{S}\int_P R^{1/3}ds, \tag{18}$$

where S is the projected area of the body on a plane normal to the direction of propagation of the incident wave and s is the arclength along the projection of shadow boundary P on that same plane.

From the basic geometry of the cylinder, the terms in Eq. (18) become

$$S = 2xl\sin\theta, \quad ds = 2\sin\theta dl, \quad R = \frac{x}{\sin^2\theta}, \tag{19}$$

where l is a unit length along the cylinder axis. Thus Q_{edge} becomes

$$Q_{edge} = \frac{c_e}{(x\sin\theta)^{2/3}}. \tag{20}$$

The angle averaging of Eq. (20) to obtain $\overline{Q}_{edge}$ is straightforward:

$$\begin{aligned}\overline{Q}_{edge} &= \frac{\int_0^{\pi/2} Q_{edge}S\sin\theta\,d\theta}{\int_0^{\pi/2} S\sin\theta\,d\theta} = \frac{2}{\sqrt{\pi}}\frac{\Gamma(7/6)}{\Gamma(5/3)}\frac{c_e}{x^{2/3}}\\ &\approx \frac{1.159595c_e}{x^{2/3}}.\end{aligned} \tag{21}$$

This universal function c_e is not known. Because c_e is independent of shape, one could accomplish this by studying the sphere alone; however, this probably produces a function that is much too complex to be included in a simple formula. We therefore use the value for optically soft particles,[10–12] $c_e^{\text{soft}} = c_0 = 0.996130$. An added complication to $\overline{Q}_{\text{edge}}$ arises, however, when we consider cylinders with small complex phases ψx. This means that for randomly oriented cylinders, $|\psi|x = 2|m-1|x \ll 1$. This occurs because what we have been calling an edge effect is in fact the field distortion around the boundaries of the particle, and hence its behavior for small phases is different from that for large phases. A simple semiempirical model of the above two behaviors is

$$\overline{Q}_{\text{edge}} = \frac{1.159595c_0}{x^{2/3} + x_{\text{crit}}},$$

$$x_{\text{crit}} = \frac{\rho_{\max}}{2|\psi|}. \tag{22}$$

Here $\rho_{\max}$ is the value of the phase at the first maximum of Q_{ext} for real indices. Thus x_{crit} is the size parameter that is approximately midway between zero and the first peak. Hence Eq. (22) is designed to have the proper asymptotic behavior for $x^{2/3} \gg x_{\text{crit}}$ and is just a constant for $x^{2/3} \ll x_{\text{crit}}$. For spheres, $\rho_{\max} \approx 4$; for randomly oriented infinite cylinders, $\rho_{\max} \approx \pi$. Thus Eq. (22) for randomly oriented infinite cylinders becomes

$$\overline{Q}_{\text{edge}} = \frac{1.159595c_0}{x^{2/3} + \pi/(4|m-1|)}. \tag{23}$$

The large-particle limit for the randomly oriented infinite cylinders becomes

$$Q_{\text{ext}} \to 2 + \overline{Q}_{\text{edge}}. \tag{24}$$

We now wish to produce a term T that, when it multiplies Eq. (17), gives the same limit as formula (24) without diverging as the size parameter goes to zero. We have found that[10] an adequate expression for our purposes is

$$T = 2 - \exp(\overline{Q}_{\text{edge}}/2). \tag{25}$$

Other orderings of the angle averaging of the anomalous diffraction and edge term expressions and their products could have been done, but complex expressions such as Eq. (14) and worse occur (see Ref. 1).

C. Extinction Formula

From the formulas in Subsections A and B, the final formula for Q_{ext} of randomly oriented infinite cylinders of medium to large size becomes

$$\left[2 + \exp(-2kx)\left(\frac{4}{3}\rho^2\left\{1 - \frac{\rho\pi}{4}\left[J_0^2\left(\frac{\rho}{2}\right) - \frac{2}{\rho}J_0\left(\frac{\rho}{2}\right)J_1\left(\frac{\rho}{2}\right) + \left(1 - \frac{2}{\rho^2}\right)J_1^2\left(\frac{\rho}{2}\right)\right]\right\} - 2\right)\right]\left[2 - \exp(\overline{Q}_{\text{edge}}/2)\right]. \tag{26}$$

This result is valid for $n \geq 1$ and $k \geq 0$.

It is of interest to derive the large ρ limit of Eq. (17), which is the backbone of formula (26) and thereby determines the peaks and valleys of the extinction curve. We do this by substituting Hankel's asymptotic expressions for the Bessel functions; see Eq. 9.2.5 in Ref. 5. The result of order $1/\rho^2$ is

$$Q_{\text{ad}}^{\text{cylinder}} \approx 2 - 4\frac{\cos\rho}{\rho} + \frac{3}{2}\left(\frac{1 - 4\sin\rho}{\rho^2}\right). \tag{27}$$

This expression is important because it is similar to the anomalous diffraction expression derived by van de Hulst[3] for spheres:

$$Q_{\text{ad}}^{\text{sphere}} = 2 - 4\frac{\sin\rho}{\rho} + 4\left(\frac{1 - \cos\rho}{\rho^2}\right). \tag{28}$$

Note that these are nearly the same, apart from an approximate phase shift of $\pi/2$ in ρ. This implies that the peaks and valleys of Q_{ext} are also shifted in the randomly oriented cylinder case by approximately $\pi/2$. Indeed, the nth peak is at approximately $2\pi(n - 1/2)$ for cylinders versus $2\pi(n - 1/4)$ for spheres. Similarly, the valleys are at approximately $2\pi n$ for cylinder versus $2\pi(n + 1/4)$ for spheres.

3. Results

The complete formula, as presented in Subsection 2.C., gives correct asymptotic behavior for both large and small $|n-1|$, $k \leq 1$, and $x \geq 1$. In studying the error behavior of the approximation, we find the midranges of $|m-1|$ and x to be of greatest interest. In this section we compare the analytic approximation with the exact randomly oriented cylinder code as implemented in IPHASE.[2]

Figure 1 shows the comparison of Q_{ext} versus x for a refractive index of $n = 1.3$, close to that of ice in the visible. It is clear that the error decreases for large x. The largest errors are near and around the first two peaks. More of the scattering physics must be considered. All the peaks or valleys, although they are well modeled, are underestimated or overestimated. This occurs because anomalous diffraction assumes that the rays are not refracted by the particle and therefore overestimates the phase difference as a function of angle. In the next section, the anomalous diffraction formulation is extended to account for this effect.

For small k and large n, one can expect a significant contribution from surface waves. This effect is

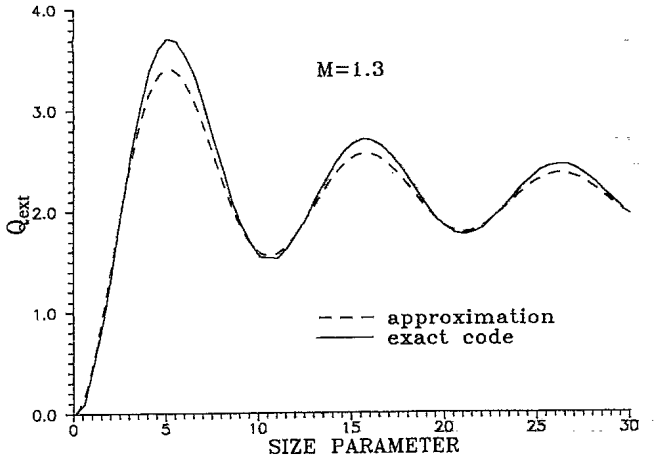

Fig. 1. Comparison between the approximation and the randomly oriented cylinder code for an index of 1.3; Q_{ext} of ice is in the visible.

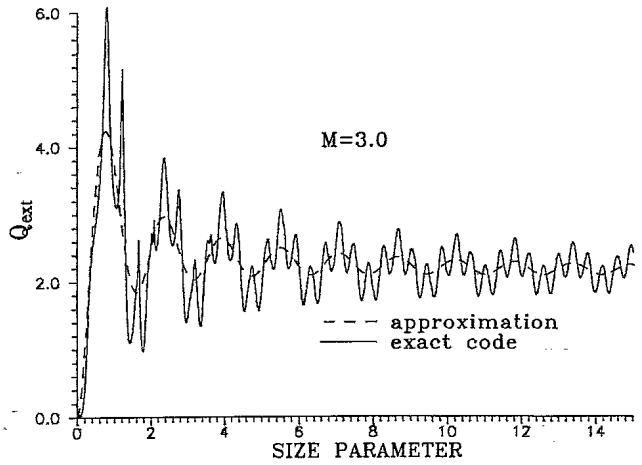

Fig. 3. Comparison between the approximation and the randomly oriented cylinder code for an index of $3 - 0i$; incipient MDR is at $x \approx 0.8$.

shown in Fig. 2 for an index of $m = 1.8 - 0i$. Unlike those for a sphere,[1] these resonant waves do not contribute as much and hence the present approximation does much better.

For large n, body resonances can occur. These are sometimes called morphology-dependent resonances (MDR's). For spheres, these occur near $nx = l\pi$, where l is a natural number. For cylinders, in any orientation, they occur at the first roots of the integer-order Bessel functions. Hence the MDR's occur when $J_l(nx) \approx 0$. For example, the first MDR occurs when $nx \approx 2.40$.

Figure 3 shows an example of an incipient MDR on the first diffraction peak of Q_{ext}. Here, $m = 3 - 0i$. Not that, despite the significant perturbation in the transition region caused by the MDR, the approximation is excellent.

The next two figures are for ice cylinders in the 3- to 5-μm and 8- to 12-μm regions, respectively. In Fig. 4 the diffraction peaks, as in the previous figures, are underestimated. Figure 5 is a case with large absorption and shows that the simple exponential damping term $\exp(-2kx)$, in Eq. (17), is quite successful in modeling the rise of the extinction.

Figure 6 represents the calculation for typical hydrosols. Many particles that are suspended in water have an absolute index of approximately 1.4. Thus the index to be considered in the scattering process is relative to water. Hence in this example $m \approx 1.4/1.33 \approx 1.05$. This is the region where anomalous diffraction applies, and the excellent agreement with the exact results in Fig. 6 testifies to this.

The last two figures in this section are for carbon fibers in the ultraviolet-to-visible and 3- to 5-μm regions. Figure 7 has an even higher absorption than that of Fig. 5 but is still well modeled. As in all the above cases for $x < 1$, we do not expect very good agreement because there has been no attempt to model the Rayleigh region. In Fig. 8 the absorption

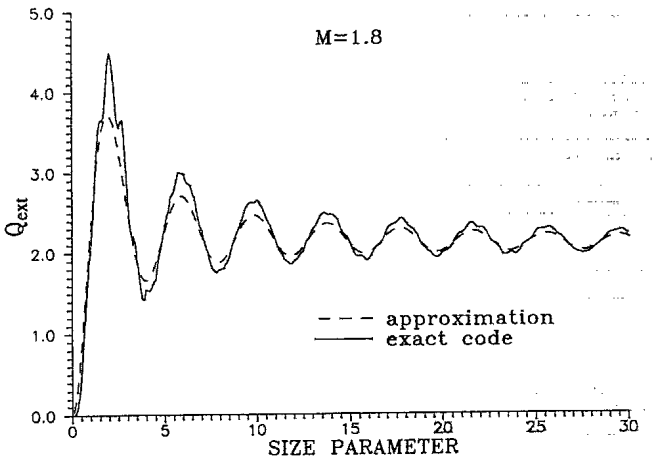

Fig. 2. Comparison between the approximation and the randomly oriented cylinder code for an index of 1.8 and an aspect ratio of 1; significant surface waves.

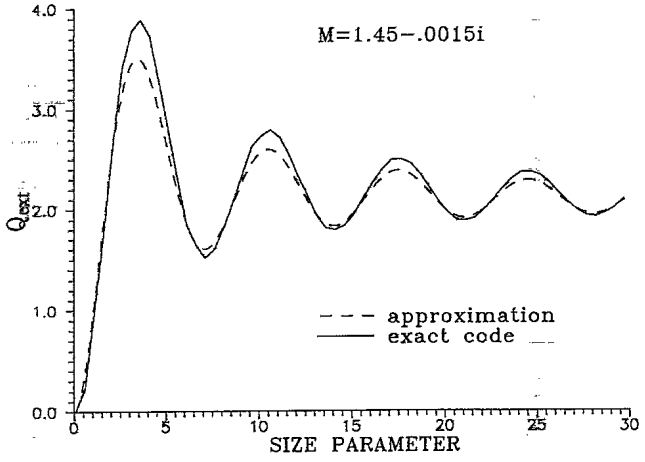

Fig. 4. Comparison between the approximation and the randomly oriented cylinder code for an index of $1.45 - 0.0015i$; Q_{ext} of ice is in the midinfrared.

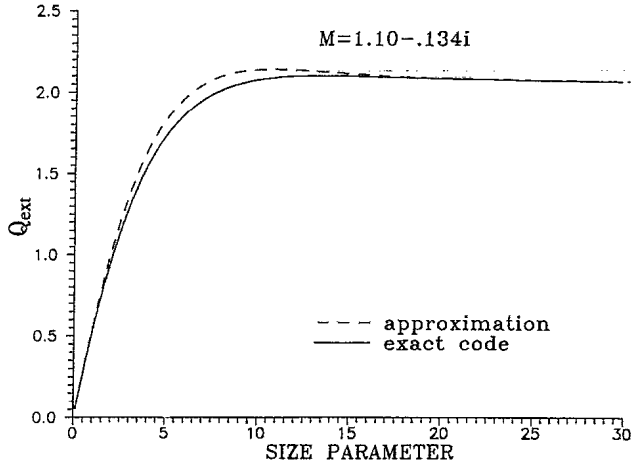

Fig. 5. Comparison between the approximation and the randomly oriented cylinder code for an index of $1.10 - 0.134i$; Q_{ext} of ice is in the far infrared.

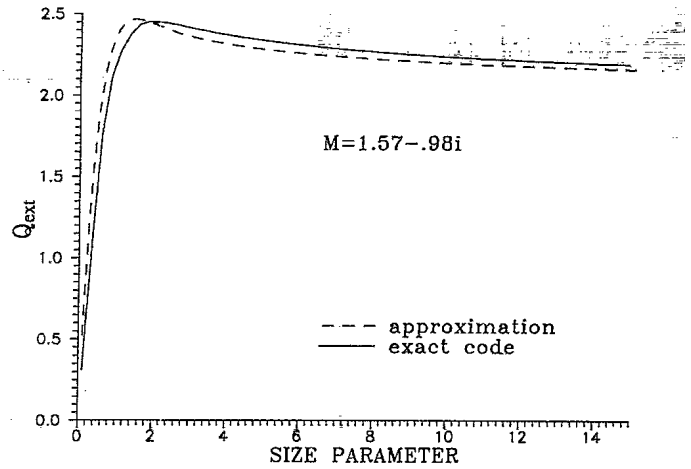

Fig. 7. Comparison between the approximation and the randomly oriented cylinder code for an index of $1.57 - 0.98i$; Q_{ext} of carbon fibers is in the ultraviolet to visible.

is extremely high and is high enough for the particle to be reflective. The overestimate of Q_{ext} for $x < 3$ is due to a breakdown of our model of the edge effect.

All our approximate Q_{ext} diagrams in this section were produced at a rate of more than 10^4 times faster than those produced by the exact code. The execution time for the approximation on an Intel *i*860 40-MHz coprocessor is approximately 70 μs and is independent of particle size and index. This large speed-up factor is essential if a complex computer model requires a large number of computations, such as in a realistic military simulation.

4. Extended Anomalous Diffraction

In Section 3 it was pointed out that the standard anomalous diffraction underestimates or overestimates the peaks or valleys in the extinction curve, because only undeviated rays are considered. In this section the extended anomalous formalism is applied first to oriented infinite cylinders; then the orientation is randomized. This approach was first used to improve the extinction formula for randomly oriented prolate spheroids.[10] This research also underlines the fact that ignoring the deviated ray produces unacceptable errors for convex elongated oriented particles.

A. Oriented Infinite Cylinders

The extended anomalous diffraction formula for oriented infinite cylinders is given by Eq. (1), except that phase difference ω now takes into account the refraction of the central ray through the cylinder

$$Q_{ad} = \pi \, \mathrm{Re}[\mathbf{H}_1(\omega) + iJ_1(\omega)], \tag{29}$$

where ω is now given by

$$\omega = \psi x = 2x[(m^2 - \cos^2\theta)^{1/2} - \sin\theta]. \tag{30}$$

Using Eqs. (20) and (22), we see that the edge term for oriented infinite cylinders in the extended anoma-

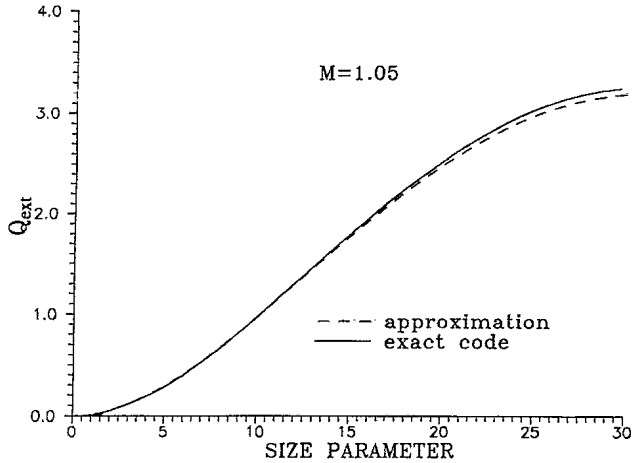

Fig. 6. Comparison between the approximation and the randomly oriented cylinder code for an index of 1.05; Q_{ext} of hydrosols is in the visible.

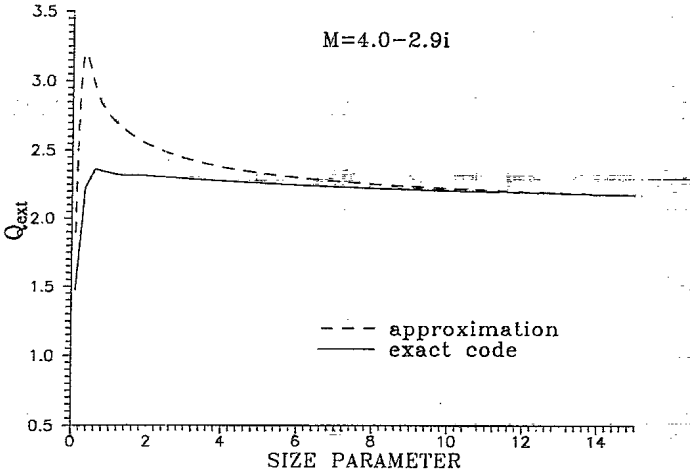

Fig. 8. Comparison between the approximation and the randomly oriented cylinder code for an index of $4 - 2.9i$; Q_{ext} of carbon fibers is in the midinfrared.

lous approximation is

$$\overline{Q}_{\text{edge}} = \frac{c_0}{(x^{2/3} + x_{\text{crit}})\sin^{2/3}\theta},$$

$$x_{\text{crit}} = \frac{3.6}{4|(m^2 - \cos^2\theta)^{1/2} - \sin\theta|}. \tag{31}$$

Because the first maximum of $\mathbf{H}_1(z)$ occurs at approximately $z = 3.6$, Eq. (31) has $\rho_{\max} = 3.6$. To be complete, Eq. (30) for the standard anomalous approach is

$$\omega = \psi x = 2x(m - 1)/\sin\theta, \tag{32}$$

and the edge term for undeviated rays is Eq. (31), but now

$$x_{\text{crit}} = \frac{3.6\sin\theta}{4|m - 1|}. \tag{33}$$

The effects of this extension on the extinction for a particular orientation can be dramatic, as shown in the next sequence of three figures. The orientation angle is decreased from 90° to 30°. For Fig. 9 there is no difference between the standard and extended anomalous diffraction approaches, because there is no deviation of the central ray. For 60°, Fig. 10, the phase of the standard anomalous diffraction solution is clearly incorrect and this error accumulates at larger x. At 30°, Fig. 11, the situation worsens. This continues for smaller orientation angles.

B. Random Orientation

In the angle-averaged case, the effects demonstrated by Figs. 9–11 can still be seen. This is shown in Figs. 12 and 13 for $m = 1.3$ and $m = 1.8$, respectively. Taking account of the deviated ray improves both the shape and amplitude of estimate Q_{ext}. This is more evident at the higher index.

Because the Jacobian, $\sin^2\theta$, weights toward 90°, the effect of ray deviation is not as dramatic as in the oriented case. Additionally, the integral produced by the angle averaging does not have an exact analytic solution. An approximate analytic formula has been obtained[13,14] but is considerably more complex than formula (26) and has an error comparable with the improvement. Hence, it is satisfactory to consider only undeviated rays in approximating Q_{ext} for random orientations if a simple efficient formula is of paramount importance.

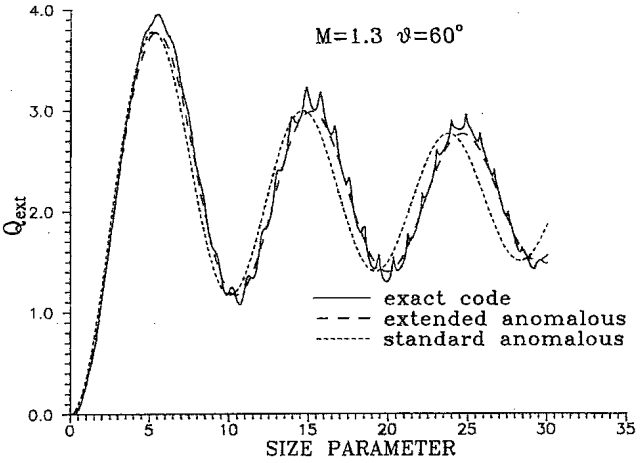

Fig. 10. Effect of extended anomalous diffraction on Q_{ext}; the index is 1.3 and the orientation angle is 60°.

5. Elliptic Infinite Cylinders: an Extension

The power of the anomalous diffraction approach can be extended in a straightforward manner to infinite cylinders of elliptical cross sections. Because the extended anomalous diffraction generally leads to complicated expressions,[1] we present only the formula for the standard anomalous diffraction. We first set up the formalism for the oriented case and then do the angle orientation.

A. Oriented Case

Let the infinite axis of the elliptic cylinder be oriented at an angle θ with respect to the direction of

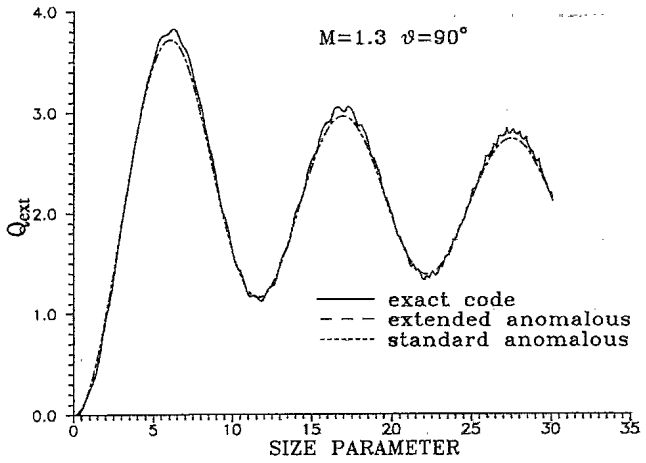

Fig. 9. Effect of extended anomalous diffraction on Q_{ext}; the index is 1.3 and the orientation angle is 90°.

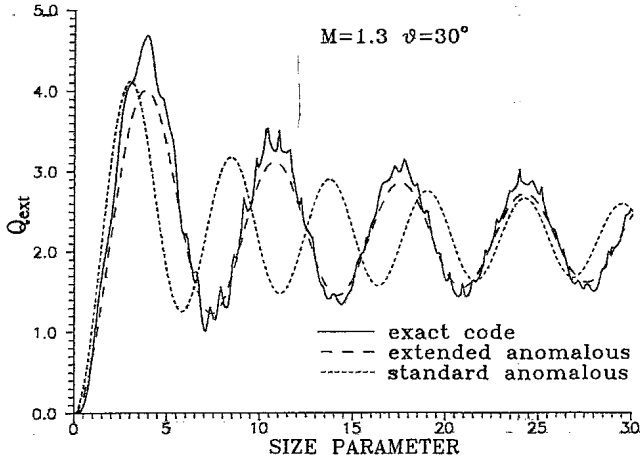

Fig. 11. Effect of extended anomalous diffraction on Q_{ext}; the index is 1.3 and the orientation angle is 30°.

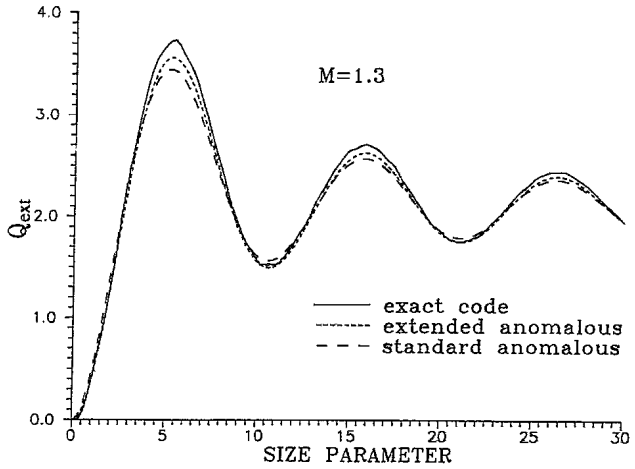

Fig. 12. Effect of extended anomalous diffraction on Q_{ext}; the index is 1.3, random orientation.

the incident radiation, as was the case for the circular cylinders. Take a cross section normal to the infinite axis of the cylinder. Let ϕ be the angle between the semimajor axis of the elliptical cross section of the cylinder and the plane defined by the direction of the incident radiation and the infinite axis of the cylinder. Let p be the projection operator of this elliptical cross section onto the shadow plane.[3] Then

$$p = (\cos^2 \phi + r^2 \sin^2 \phi)^{1/2}, \tag{34}$$

where r is the ratio of semimajor axis size parameter a to semiminor axis size parameter b of the elliptic cross section. Anomalous diffraction expression Q_{ad} for an infinite elliptical cylinder oriented at angles θ and ϕ is

$$Q_{ad} = \pi \, \mathrm{Re}[\mathbf{H}_1(\alpha) + iJ_1(\alpha)], \tag{35}$$

where α is given by

$$\alpha = \frac{2(m-1)rb}{p \sin \theta}. \tag{36}$$

Thus Q_{ad} is the same as for the circular cylinder but with x replaced by rb/p. The edge term is simply derived to be

$$Q_{edge} = \frac{c_0}{p^2}\left(\frac{r}{b \sin \theta}\right)^{2/3}. \tag{37}$$

These equations allow us to study the randomly oriented case.

B. Random Orientation

The angle averaging must be done over two angles, θ and ϕ. It is evident that the averaging over θ will give formula (26) with $\rho \rightarrow 2(n-1)rb/(p \sin \theta)$, $x \rightarrow rb/p$, and

$$\overline{Q}_{edge} = \frac{1.159595 c_0 r^{2/3}}{p^2[b^{2/3} + \pi/(4|m-1|)]}. \tag{38}$$

This leaves the angle averaging over ϕ to be performed. An analytic expression can be found, but it is complicated. However, it can be numerically integrated or approximated in various limits. The latter is discussed in Subsection 5.C.

Figures 14 and 15 are computations of the extinction efficiency predicted by standard anomalous diffraction plus edge term for randomly oriented elliptic cylinders. Figure 14 compares the results between a circular cylinder and elliptic cylinder with $r = 2$. Figure 15 is the same but $r = 3$ for the elliptic cylinder. Note that the peaks are shifted toward smaller b and the amplitudes are reduced with increasing r. Most of the peak shift occurs between $r = 1$ and $r = 2$.

C. Approximations

If we make the same substitution, as was done in Subsection 5.B. but into the asymptotic form of formula (27), and then we perform an approximate angle averaging over the first terms only, we obtain a simple and reasonably accurate expression for the

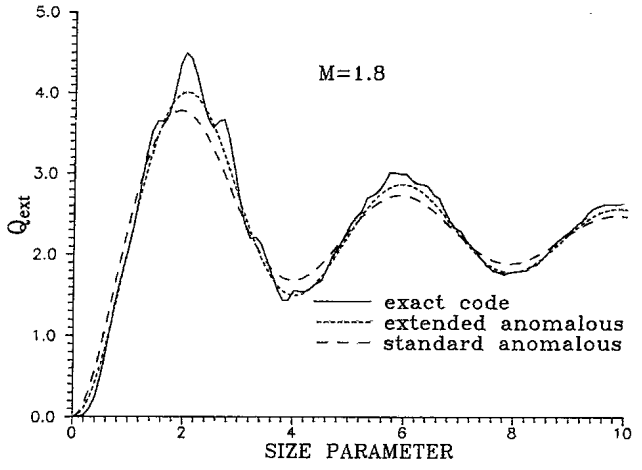

Fig. 13. Effect of extended anomalous diffraction on Q_{ext}; the index is 1.8, random orientation.

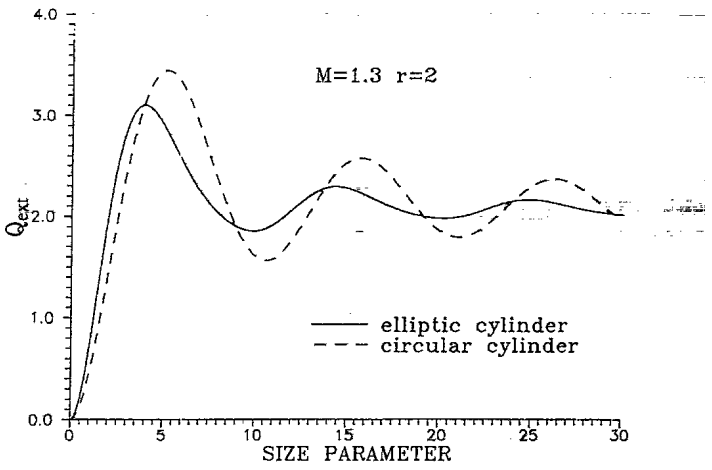

Fig. 14. Comparison between the randomly oriented circular cylinders and elliptic cylinders. The index is 1.3 and $r = 2$.

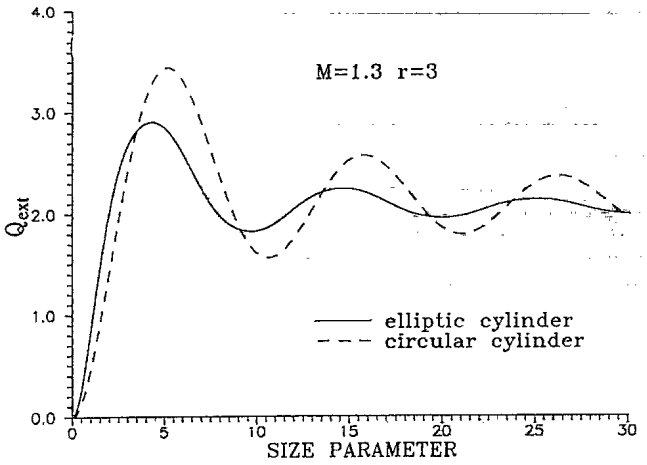

Fig. 15. Comparison between the randomly oriented circular cylinders and elliptic cylinders. The index is 1.3 and $r = 3$.

extinction efficiency. Thus the completely angle-averaged extinction efficiency, $\langle Q_{ad}\rangle$, is approximately

$$\langle Q_{ad}\rangle \approx 2 - \frac{4}{E(\epsilon^2)}\int_0^{\pi/2}\frac{\cos(\alpha r/p)}{\alpha r}p^2 d\phi, \tag{39}$$

where $E(\epsilon^2)$ is the complete elliptic integral of the second kind, $\epsilon^2 = 1 - 1/r^2$ is the square of the eccentricity, and $\alpha = 2(n-1)b$.

The integral in the second term of formula (39) must be approximated. By rewriting $p = [\cos^2(\phi) + r^2\sin^2(\phi)]^{1/2}$ as $r[1 - \epsilon^2\cos^2(\phi)]^{1/2} = rp'$, we can expand $1/p$ in terms of ϵ^2, which is always between zero and one and hence small. Thus

$$\frac{1}{p} \approx \frac{1}{r}[1 + f(\epsilon^2)\cos^2(\phi)]. \tag{40}$$

If the Taylor expansion is used then $f(\epsilon^2) = \epsilon^2/2$. This function, as is shown later, can be better optimized.

Putting formula (40) into the integral in formula (39), we get

$$\int_0^{\pi/2}\frac{\cos(\alpha r/p)}{\alpha r}p^2 d\phi \approx \frac{1}{\alpha}\int_0^{\pi/2}\cos[\alpha[1 + f(\epsilon^2)\cos^2(\phi)]] \times [1 - \epsilon^2\cos^2(\phi)]d\phi. \tag{41}$$

After some significant algebra the evaluation of formula (41) requires the performance of the following integrals:

$$I_1 = \int_0^{\pi/2}\cos[2\beta\cos^2(\phi)]d\phi = \frac{\pi}{2}\cos(\beta)J_0(\beta), \tag{42}$$

$$I_2 = \int_0^{\pi/2}\sin[2\beta\cos^2(\phi)]d\phi = \frac{\pi}{2}\sin(\beta)J_0(\beta), \tag{43}$$

$$I_3 = \int_0^{\pi/2}\cos[2\beta\cos^2(\phi)]\cos^2(\phi)d\phi = \frac{\pi}{4}{}_2F_3\left[\begin{matrix}3/4, 5/4\\ 1/2, 1, 3/2\end{matrix}\middle| -\beta^2\right] = \frac{\pi}{4}[\cos(\beta)J_0(\beta) - \sin(\beta)J_1(\beta)], \tag{44}$$

$$I_4 = \int_0^{\pi/2}\sin[2\beta\cos^2(\phi)]\cos^2(\phi)d\phi = \frac{3\pi\beta}{8}{}_2F_3\left[\begin{matrix}5/4, 7/4\\ 3/2, 3/2, 2\end{matrix}\middle| -\beta^2\right] = \frac{\pi}{4}[\sin(\beta)J_0(\beta) + \cos(\beta)J_1(\beta)]. \tag{45}$$

In Eqs. (42)–(45), I_1 to I_4 can be obtained by the use of MATHEMATICA V.2.2.[15] The reduction of the two ${}_2F_3$ hypergeometric functions in I_3 and I_4 requires breaking them into their even and odd parts (MacRobert's theorem) and then using the reduction tables.[8]

Putting these results into formula (39), we finally obtain

$$\langle Q_{ad}\rangle \approx 2 - \frac{2\pi}{E(\epsilon^2)}\left\{\frac{\cos(\alpha)}{\alpha}\left[\left(1 - \frac{\epsilon^2}{2}\right) \times \cos(\beta)J_0(\beta) + \frac{\epsilon^2}{2}\sin(\beta)J_1(\beta)\right]\right. \tag{46}$$

$$\left. - \frac{\sin(\alpha)}{\alpha}\left[\left(1 - \frac{\epsilon^2}{2}\right)\sin(\beta)J_0(\beta) - \frac{\epsilon^2}{2}\cos(\beta)J_1(\beta)\right]\right\}, \tag{47}$$

where $\beta = \alpha f(\epsilon^2)$.

We still must determine an optimal form for $f(\epsilon^2)$. A simple but effective approach is to minimize the least-squares error, $\mathscr{E}$, of $1/p$ or $1/p'$ and formula (40), i.e.,

$$\mathscr{E} = \min\left(\int_0^{\pi/2}[[1 + f(\epsilon^2)\cos^2(\phi)](p')^2 - p']^2 d\phi\right). \tag{48}$$

Thus

$$\frac{\partial\mathscr{E}}{\partial f} = 2\int_0^{\pi/2}[[1 + f(\epsilon^2)\cos^2(\phi)](p')^2 - p'] \times \cos^2(\phi)(p')^2 d\phi = 0. \tag{49}$$

Solving for f we get

$$f(\epsilon^2) = \left[\int_0^{\pi/2}(p')^3\cos^2(\phi)d\phi - \int_0^{\pi/2}(p')^4\cos^2(\phi)d\phi\right] \Big/ \int_0^{\pi/2}(p')^4\cos^4(\phi)d\phi \equiv (I_5 - I_6)/I_7. \tag{50}$$

The above three integrals, I_5 to I_7, can be solved again by the use of MATHEMATICA and the Gauss contiguity relations.[5] Thus

$$I_5 = \int_0^{\pi/2} (p')^3 \cos^2(\phi) d\phi = \frac{\pi}{4} {}_2F_1\left[\begin{matrix}-3/2, 3/2 \\ 2\end{matrix}\middle| \epsilon^2\right]$$

$$= \frac{1}{15\epsilon^2}[(3 - 7\epsilon^2 + 4\epsilon^4)K(\epsilon^2) - (3 - 13\epsilon^2 + 8\epsilon^4)E(\epsilon^2)]$$

$$\approx \frac{\pi}{2(4 - \epsilon^2)}\left[2 + \left(\frac{4}{5\pi} - 3\right)\epsilon^2 + \epsilon^4\right], \quad (51)$$

$$I_6 = \int_0^{\pi/2} (p')^4 \cos^2(\phi) d\phi$$

$$= \frac{\pi}{8}\left(2 - 3\epsilon^2 + \frac{5}{4}\epsilon^4\right), \quad (52)$$

$$I_7 = \int_0^{\pi/2} (p')^4 \cos^4(\phi) d\phi$$

$$= \frac{\pi}{16}\left(3 - 5\epsilon^2 + \frac{35}{16}\epsilon^4\right). \quad (53)$$

Here $K(\epsilon^2)$ is the complete elliptic integral of the first kind. The approximation in formula (51) is a rational approximation with matched asymptotes to simplify the computation if required. This gives a rational form for $f(\epsilon^2)$ that is very close to the Taylor solution for $\epsilon \to 0$. It is nearly a factor of 2 larger than the Taylor solution, however, when $\epsilon \to 1$, and hence it is where we expect the greatest improvement in $\langle Q_{ad} \rangle$.

A second approximation, which is good for small ϵ^2, can be obtained by a Taylor expansion of $\langle Q_{ad} \rangle$ near $\epsilon^2 = 0$, i.e.,

$$\langle Q_{ad}(\epsilon^2) \rangle = \langle Q_{ad}(0) \rangle + \epsilon^2 \left.\frac{\partial \langle Q_{ad}(\epsilon^2) \rangle}{\partial \epsilon^2}\right|_{\epsilon^2=0} + \cdots. \quad (54)$$

This expansion is restricted not only to small ϵ^2 but also to small b because the phase information in $\langle Q_{ad} \rangle$ is also being approximated. With some algebraic manipulation, the second term on the right-hand side becomes

$$\left.\frac{\partial \langle Q_{ad}(\epsilon^2) \rangle}{\partial \epsilon^2}\right|_{\epsilon^2=0} = \frac{\alpha^2}{3} - \frac{\pi\alpha^3}{16}\left\{{}_1F_2\left[\begin{matrix}1/2 \\ 2, 3\end{matrix}\middle| -\frac{\alpha^2}{4}\right] - \frac{\alpha^2}{48} {}_1F_2\left[\begin{matrix}3/2 \\ 3, 4\end{matrix}\middle| -\frac{\alpha^2}{4}\right]\right\} + \frac{1}{4}\langle Q_{ad}(0) \rangle. \quad (55)$$

Hence, with additional work, the approximation to $\langle Q_{ad}(\epsilon^2) \rangle$ for small ϵ^2 and b becomes

$$\langle Q_{ad}(\epsilon^2) \rangle \approx \left(1 + \frac{\epsilon^2}{2}\right)\langle Q_{ad}(0) \rangle - \frac{\pi\epsilon^2\alpha}{2} J_1{}^2\left(\frac{\alpha}{2}\right)$$

$$= \left(1 + \frac{\epsilon^2}{2}\right)\frac{4\alpha^2}{3}\left\{1 - \frac{\pi\alpha}{4}\left[J_0{}^2\left(\frac{\alpha}{2}\right) - \frac{2}{\alpha} J_0\left(\frac{\alpha}{2}\right) J_1\left(\frac{\alpha}{2}\right) + \left(1 - \frac{2}{\alpha^2}\right) J_1{}^2\left(\frac{\alpha}{2}\right)\right]\right\} - \frac{\pi\epsilon^2\alpha}{2} J_1{}^2\left(\frac{\alpha}{2}\right). \quad (56)$$

We can obtain an additional approximation by taking a formal asymptotic expansion[16] of formula (27). Following formulas (6.3.28) and (6.3.38) of Ref. 16, we get

$$\langle Q_{ad} \rangle \approx 2 - \frac{2}{\alpha E(\epsilon^2)}\left(\frac{2\pi}{\epsilon^2\alpha}\right)^{1/2}\left[(1 - \epsilon^2)^{7/4}\cos\left(\frac{\alpha}{\sqrt{1 - \epsilon^2}} - \frac{\pi}{4}\right) + \cos\left(\alpha + \frac{\pi}{4}\right)\right] + \frac{1}{\alpha^2 E(\epsilon^2)} \times \left\{(2 - \epsilon^2)E(\epsilon^2) - \frac{1 - \epsilon^2}{2} K(\epsilon^2) - 3\left(\frac{2\pi}{\epsilon^2\alpha}\right)^{1/2}\left[(1 - \epsilon^2)^{9/4}\sin\left(\frac{\alpha}{\sqrt{1 - \epsilon^2}} - \frac{\pi}{4}\right) + \sin\left(\alpha + \frac{\pi}{4}\right)\right]\right\}. \quad (57)$$

This formula is asymptotic in α and ϵ. It is clear that as ϵ goes to zero, formula (57) does not go to asymptotic circular cylinder formula (27). We can easily correct this by multiplying the relevant terms in formula (57) by $1 - \exp(-\sqrt{\pi\epsilon^2\alpha}/2)$. The result is

$$\langle Q_{ad} \rangle \approx 2 + \frac{1}{\alpha^2 E(\epsilon^2)}\left[(2 - \epsilon^2)E(\epsilon^2) - \frac{1 - \epsilon^2}{2} K(\epsilon^2)\right] - [1 - \exp(-\sqrt{\pi\epsilon^2\alpha}/2)]\frac{1}{\alpha E(\epsilon^2)}\left(\frac{2\pi}{\epsilon^2\alpha}\right)^{1/2} \times \left\{2\left[(1 - \epsilon^2)^{7/4}\cos\left(\frac{\alpha}{\sqrt{1 - \epsilon^2}} - \frac{\pi}{4}\right) + \cos\left(\alpha + \frac{\pi}{4}\right)\right] + \frac{3}{\alpha}\left[(1 - \epsilon^2)^{9/4}\sin\left(\frac{\alpha}{\sqrt{1 - \epsilon^2}} - \frac{\pi}{4}\right) + \sin\left(\alpha + \frac{\pi}{4}\right)\right]\right\}, \quad (58)$$

This formula is now asymptotic in α, for any ϵ.

Figure 16 is a comparison between the numerically calculated $\langle Q_{ad} \rangle$ and formula (58). The numerical integration was carried out by the use of a

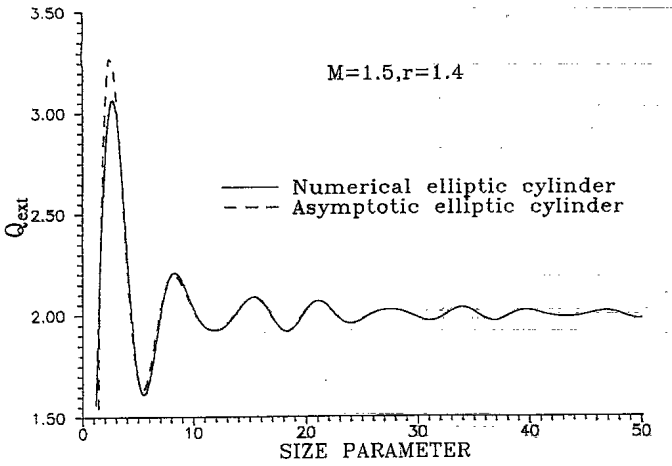

Fig. 16. Comparison between numerically integrated $\langle Q_{ad} \rangle$ and formula (58). The index is 1.5 and $r = 1.4$ (note that $\alpha = b$).

256-point Gaussian quadrature. It is surprising that such a simple expression as formula (58) can capture all of the subtle features of the oscillations. This formula makes it obvious that the extinction peaks for large aspect cylinders occur near $\pi(n - 1/4)$. This formula forms an excellent backbone to $\langle Q_{ext} \rangle$. All that remains is to add the effects of absorption and the edge terms in a manner similar to that done for circular cylinders. Hence, the addition of absorption is performed as in Eq. (17). All that is required is the following simple integration to obtain the averaged absorption length λ:

$$\lambda = \frac{1}{E(\epsilon^2)} \int_0^{\pi/2} \left(\frac{2kb}{p'}\right) p' \mathrm{d}\phi = \frac{\pi k b}{E(\epsilon^2)}. \tag{59}$$

The edge term also requires just a simple integration. We set it up by using Eq. (38) and changing the x_{crit}, $\pi/(4|m - 1|)$ by the semiempirical form $\pi(1 - \epsilon^2/4)/(4|m - 1|\, b)$. See the discussion concerning Eq. (22).

$$\langle Q_{edge} \rangle = \frac{1.159595 c_0}{r^{4/3}[b^{2/3} + \pi(1 - \epsilon^2/4)/(4|m - 1|)]E(\epsilon^2)} \times \int_0^{\pi/2} \left[\frac{1}{(p')^2}\right] p' \mathrm{d}\phi = \frac{1.159595 c_0}{r^{4/3}[b^{2/3} + \pi(1 - \epsilon^2/4)/(4|m - 1|)]} \frac{K(\epsilon^2)}{E(\epsilon^2)}. \tag{60}$$

Thus, the asymptotic formula for $\langle Q_{ext} \rangle$ is

$$\langle Q_{ext} \rangle \approx [2 - \exp(-\lambda)(\langle Q_{ad} \rangle - 2)][1 - \exp(-\langle Q_{edge} \rangle/2)]. \tag{61}$$

Unfortunately, the accuracy of formula (61) cannot at present be determined because there are no known results for randomly oriented elliptic cylinders. The results to date are for a particular orientation only (see Ref. 17 and references therein).

6. Conclusions and Limitations

We have presented an analytic approximation to Q_{ext} for oriented and randomly oriented infinite cylinders of circular cross section. In addition, a formula requiring only one numerical integration is given for randomly oriented infinite cylinders of elliptic cross section. Various asymptotic expressions for these formulas are also developed.

The large size regime is modeled by anomalous diffraction plus edge or Fock terms as in Ref. 1. The small particle size limit, although roughly modeled, is not treated extensively because the resulting formulas would be too complex. Furthermore, at least in the case of circular infinite cylinders, the exact code is efficient in this regime.

An extension to the anomalous diffraction approach, similar to that in Ref. 1, is also developed for the case of circular cylinders. This demonstrates that this extended anomalous diffraction is significant only when the cylinders are oriented.

The circular cylinder formula gives good results with little loss in accuracy for medium to large size parameters for $n \geq 1$ and $0 \leq k \leq 3$ and, for elliptic cylinders, for modest aspect ratios ($r \leq 4$). Typical errors of approximately 5% or less are encountered in the circular cylinder case. The errors observed have the same behavior as those previously seen for randomly oriented spheroids.[1] Errors for the elliptic cylinder cannot be determined at this date because there are no known exact results.[17] However, there is no physical reason we know of that would make the errors in the formulas behave differently for elliptical cylinders than those of either the circular cylinders or spheroids.

If high precision is not required, the circular cylinder formula is far more economical in computer time than the exact random infinite cylinder code. This is even more true when elliptical cylinders or polydispersions are considered. Taking account of both the range of demonstrated validity and the accuracy, we believe the circular cylinder formula is superior to all other approximations known by us.

An even simpler form for large optical sizes is also derived for both the circular and elliptic cylinders, which are analogs of Van de Hulst's famous formula for spheres. This allows for the simple determination of the maxima and minima of the extinction.

The results of this study demonstrate, once again, the effectiveness of the combined approaches of anomalous diffraction and edge effect terms in modeling the extinction from smooth convex bodies. This is a positive signal toward further research on other shapes and scattering properties to cover fully the broad spectrum of natural and artificial scatterers.

References

1. B. T. N. Evans and G. R. Fournier, "Analytic approximation to randomly oriented spheroid extinction," Appl. Opt. **33,** 5796–5804 (1994).
2. B. T. N. Evans, "An interactive program for estimating extinction and scattering properties of most particulate clouds," MRL Rep. R-1123/88 (Materials Research Laboratory, Melbourne, Australia, 1988).
3. H. C. Van de Hulst, *Light Scattering by Small Particles,* 1st ed. (Wiley, New York, 1957).
4. G. L. Stephens, "Scattering of plane waves by soft obstacles: anomalous diffraction theory for circular cylinders," Appl. Opt. **23,** 954–959 (1984).
5. M. Abramowitz and I. A. Stegun, eds., *Handbook of Mathematical Functions,* 8th ed. (Dover, New York, 1972).
6. A. P. Prudnikov, Y. A. Brychkov, O. I. Marichev, *Tables of Integrals and Series Vol. 3: More Special Functions* (Gordon & Breach, London, 1990).
7. A. Erdélyi, W. Magnus, F. Oberhettinger, and F. G. Tricomi, *Tables of Integral Transforms* (McGraw-Hill, New York, 1954), Vol. II.
8. Y. L. Luke, *The Special Functions and Their Approximations* (Academic, New York, 1969), Vols. I and II.
9. D. S. Jones, "High-frequency scattering of electromagnetic waves," Proc. R. Soc. London Ser. A **240,** 206–213 (1957).
10. G. R. Fournier and B. T. N. Evans, "Approximation to extinction efficiency for randomly oriented spheroids," Appl. Opt. **30,** 2042–2048 (1991).
11. H. M. Nussenzveig and W. J. Wiscombe, "Efficiency factors in Mie scattering," Phys. Rev. Lett. **45,** 1490–1494 (1980).
12. V. P. Beckmann and W. Franz, "Berechnung der Streuquerschnitte von Kugel und Zylinder unter Anwendung einer modifizierten Watson-Transformation," Z. Naturforsch. **12a,** 533–537 (1957).
13. B. T. N. Evans and G. R. Fournier, "A procedure for obtaining an algebraic approximation to certain integrals," DREV Rep. R-4653/91 (Defense Research Establishment Valcartier, Courcelette, Quebec, Canada, 1991).
14. B. T. N. Evans and G. R. Fournier, "Algebraic approximation to some integrals in optics," J. Phys. A **26,** 647–663 (1993).
15. S. Wolfram, *Mathematica: a System for Doing Mathematics by Computer* (Addison-Wesley, New York, 1989).
16. N. Bleistein and R. A. Handelsman, *Asymptotic Expansions of Integrals* (Dover, New York, 1986).
17. C. S. Kim and C. Yeh, "Scattering of an obliquely incident wave by a multilayered elliptical lossy dielectric cylinder," Radio Sci. **26,** 1165–1176 (1991).